

## Experimental Evidence of Thermophoresis of Non-Brownian Particles in Pure Liquids and Estimation of Their Thermophoretic Mobility

Anne Regazzetti, Mauricio Hoyos, and Michel Martin\*

*Ecole Supérieure de Physique et de Chimie Industrielles, Laboratoire de Physique et Mécanique des Milieux Hétérogènes (UMR CNRS 7636), 10 Rue Vauquelin, 75231 Paris Cedex 05, France*

*Received: December 15, 2003; In Final Form: June 25, 2004*

The first experimental evidence that noncolloidal particles exhibit a thermophoretic migration when placed in a temperature gradient is provided by observing the retention of micron-sized porous spherical particles, used as packing in liquid chromatography, in a thermal field-flow fractionation instrument. To eliminate the perturbing gravitational effects, the channel flow is set vertically and the temperature gradient horizontally. A method of determination of the thermophoretic mobility is developed. It relies on the dependence of the amount of retained particles on the duration of the initial stop-flow step immediately after sample introduction. This method may be implemented for the determination of particle mobility with any kind of applied force field. The value of the thermophoretic mobility is found to depend on the chemical nature of the particle surface, but not significantly on the nature of the pure suspending liquid. For silica particles, it is slightly larger in water than in acetonitrile. In this latter liquid, the thermophoretic mobility of pure silica particles is about 3 times larger than that of octadecyl-bonded silica particles. This demonstrates that, for micron-sized particles, thermophoresis is governed by surface effects and may be the basis of a process for characterizing the surface properties of particulate materials.

### Introduction

When a temperature gradient is applied across a mixture of two or more substances, a concentration nonuniformity appears. This phenomenon is called thermal diffusion, or thermodiffusion, or still Soret effect. It has been observed first in liquids,<sup>1–4</sup> then in gases,<sup>5</sup> and in polymer solutions.<sup>6</sup> This thermodiffusion process is at the basis of the separation of gases,<sup>7</sup> liquids,<sup>8</sup> and polymers<sup>6</sup> by means of the thermogravitational column. More recently, this process was exploited for the separation of polymer solutions by thermal field-flow fractionation. This technique belongs to the family of field-flow fractionation (FFF) methods of separation of macromolecular, colloidal, and particulate materials developed by Giddings.<sup>9</sup> It relies on the use of a temperature gradient, perpendicular to the flow axis of a carrier liquid, to induce differential migration of the various macromolecular components of the injected sample. Theoretical models of the migration process in the thermal FFF channel allow the extraction of the Soret coefficients,  $S_T$ , of the analyzed species from their experimental residence times.<sup>10,11</sup> As  $S_T$  is the ratio of the thermodiffusion coefficient,  $D_T$ , to the mass diffusion coefficient,  $D_m$ ,  $D_T$  can be determined if  $D_m$  is known. The method was applied to the study of the dependence of the Soret and thermodiffusion coefficients of polymers and copolymers on their structural characteristics (such as molar mass, chemical composition, branching).<sup>12</sup>

Because FFF methods are well suited for the analysis of macromolecules of very large molar masses and of particulate suspensions, the behavior of colloidal suspensions in thermal FFF was investigated. Evidence that colloidal particles suspended in liquids exhibit a thermophoretic migration was previously provided by the pioneering work of McNab and

Meisen on polystyrene (PS) latex colloids.<sup>13</sup> Thermal FFF experiments confirmed this evidence<sup>14,15</sup> and demonstrated it for other kinds of latex and colloidal particles, such as silica,<sup>14</sup> polybutadienes,<sup>16,17</sup> poly(methyl methacrylate)s, silanized silica, styrene-vinylbenzyl chloride copolymer latex, and, even, palladium particles,<sup>17</sup> before it was observed by forced Rayleigh scattering<sup>18,19</sup> and the thermogravitational column method.<sup>20</sup> Later on, the effect was demonstrated for other types of particles, core-shell latex,<sup>21</sup> acrylonitrile-butadiene-styrene plastic, rubber,<sup>22</sup> modified silica,<sup>23</sup> styrene-butyl methacrylate latex,<sup>24</sup> and metal (silver, gold, platinum)<sup>25</sup> particles. The influence of various operational parameters on  $D_T$  was investigated in several of these studies (see also ref 26).

The same experimental method, thermal FFF, was used for investigation of the behavior of solutions of polymers and of suspensions of colloidal particles undergoing a temperature gradient, and the same retention data interpretation procedure was applied to obtain the  $D_T$  coefficients of both kinds of species. This illustrates the phenomenological continuity in the effect exerted by a temperature gradient on the mixture of a liquid and another component as one goes from small molecules to large particles. Traditionally, the effect for small molecules (or solutions) is called thermodiffusion, while for suspensions of particles in gases or in liquids it is called thermophoresis. This is a phoretic migration induced by a temperature gradient. Thus, the thermodiffusion coefficient,  $D_T$ , can also be called thermophoretic mobility (it is the thermophoretic velocity, impelled on the species by the temperature gradient, per unit value of this temperature gradient).

The experimental activity on thermophoresis in liquids prompted theoretical investigations on this process. McNab and Meisen<sup>13</sup> found that their  $D_T$  values were related to particle and liquid properties (thermal conductivities of particle and liquid, liquid density, and viscosity) by an expression similar to

\* Corresponding author. Tel: +33-1-4079-4707. Fax: +33-1-4079-4523. E-mail: martin@pmmh.espci.fr.

Epstein's gas equation.<sup>27</sup> However, as noted by Anderson,<sup>28</sup> the theory of thermophoresis in gases, which is well understood from the kinetic theory of gases and relies on the collisions between gas molecules and particle surface, is not appropriate for describing thermophoresis in liquids, since the liquid state is dominated by intermolecular potential energies rather than by kinetic exchange of momentum. All theories developed for thermophoresis in liquids consider it as an interfacial effect, similar to that observed in electrophoresis or diffusiophoresis when an electrical field or a concentration gradient, respectively, instead of a temperature gradient, is applied to the suspension.<sup>28,29</sup> Semenov and co-workers have developed several theories of thermophoresis of particles.<sup>30–34</sup> The differences noted between some of these theories are somewhat obscure. Nevertheless, they all convey the idea that thermophoresis is linked to the distribution of substances added to the liquid for stabilizing the suspension (such as electrolyte ions or surfactant molecules) as a result of their interactions with the particles (steric, electrostatic, van der Waals interactions) in a thin layer around each particle. This distribution is modified by the applied temperature gradient. This results in an excess osmotic pressure gradient, which induces the particle movement in the liquid. Similar theoretical approaches were more recently developed.<sup>35,36</sup> The theory for thermophoresis for latex particles, which are emulsions of droplets of polymer solution in a polar solvent, is derived from the distribution of the mers of the polymer chains partitioning between the droplets and the surrounding polar solvent.<sup>34</sup> The theories predict that, in a surfactant solution, the particles should move toward the cold regions. In the case of electrolyte solutions, the direction of migration may change with the electrolyte concentration, depending on the shape of the potential energy distribution curve around a particle. Recently, Semenov presented a theoretical model of particle thermophoresis in pure liquids. It is based on the concentration distribution of the molecules of the liquid in a thin layer around a particle arising from their dipole–dipole interactions with the particle. These interactions are accounted for by the Hamaker constant.<sup>37</sup>

Most experiments on thermophoresis of particles in liquids have concerned submicron particles. They provide clear evidence of the thermophoretic migration of Brownian particles. One may wonder if such a migration can also be observed for non-Brownian particles. Indeed, the above-discussed theories associate particle thermophoresis in liquids to the presence of an interfacial layer around the particles. It is questionable whether such an effect, like other interfacial colloidal effects, remains significant when the interfacial layer thickness becomes increasingly smaller than the particle size. The few experiments on micron-sized particles have been performed with PS latex particles.<sup>13,15,16,38</sup> The 1.01  $\mu\text{m}$  particles used by McNab and Meisen were just at the outer of the submicron domain, which is classically considered as the Brownian domain. In fact, this domain can be considered as that for which the time of diffusion of a particle over one particle diameter is less than that of convection by sedimentation over that distance (i.e., for which the Peclet number is smaller than 1). Thus, the 1.01  $\mu\text{m}$  PS latex particles are Brownian ( $Pe \approx 0.06$ ). This is not the case for the other micron-sized particles analyzed by thermal FFF. However, in FFF experiments, the forces exerted by the applied field on micron-sized particles are balanced by hydrodynamic lift forces, rather than by Brownian diffusion, as is generally the case for submicron particles. Because the lift forces are poorly characterized, it is not possible to derive the  $D_T$  values of micron-sized particles from their thermal FFF retention.

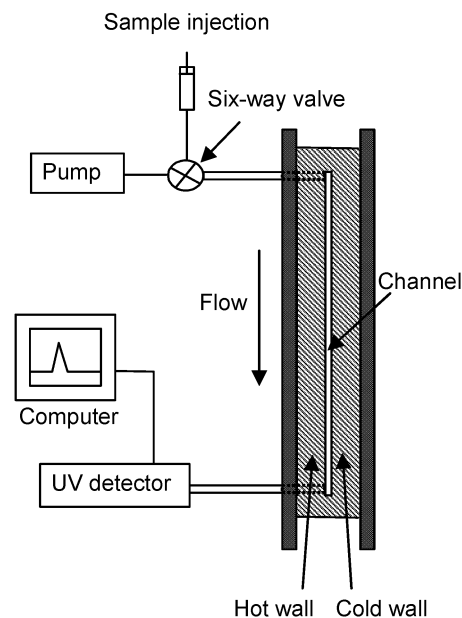


**Figure 1.** Schematic diagram of the thermal FFF instrument.

Furthermore, all previous experiments on thermal FFF of micron-sized particles have been performed in a horizontal channel, so that gravitational forces affect the particle behavior. It was shown that these forces allow the separation of micron-sized PS latex particles without applying an additional field.<sup>39,40</sup> It is therefore not possible to positively conclude about the existence of a thermophoretic migration of micron-sized particles in a horizontal thermal FFF channel from the sole observation that these particles are retained.

Other experimental methods have been sought for investigating the thermophoresis of such particles, such as the forced Rayleigh scattering method, the optical beam deflection method, or the thermogravitational column. However, it seems that the perturbations arising from the ubiquitous gravitational sedimentation are too strong to allow any definitive conclusion. In the present study, a thermal FFF channel is used in an unconventional way to study the behavior of non-Brownian particles under a temperature gradient.

## Experimental Section

A sketch of the experimental setup is shown in Figure 1. The thermal FFF channel used in this study has been described previously.<sup>41</sup> It had a tip-to-tip length of 46 cm, a breadth of 1.8 cm, and a thickness of 0.1 mm. The carrier liquid was introduced at a constant flow rate, provided by a syringe pump (Model A-99, Razel Scientific Instruments, Stamford, CT), at the upstream end of the channel. Sample injection was made by means of a six-port homemade injection valve equipped with a 20  $\mu\text{L}$  sample loop. The effluent was fed to a flow-through UV photometer (Model 2138 Uvicord S, LKB, Bromma, Sweden), operating at a wavelength of 254 nm, by means of a Teflon connection tube at the downstream end of the channel. The detector signal was recorded on a computer using a data acquisition board (Model DAS-801, Keithley, Taunton, MA). The temperatures,  $T_h$  and  $T_c$ , of the hot and cold plates were selected by controlling the voltage of cartridge heaters in the hot plate and flow of tap water through the cold plate, respectively.

Two kinds of particles were used in this study, Hypersil 3  $\mu\text{m}$  and Hypersil-ODS 3  $\mu\text{m}$ , kindly gifted by Thierry Domenger (Thermo-Electron, Courtabœuf, France). They are

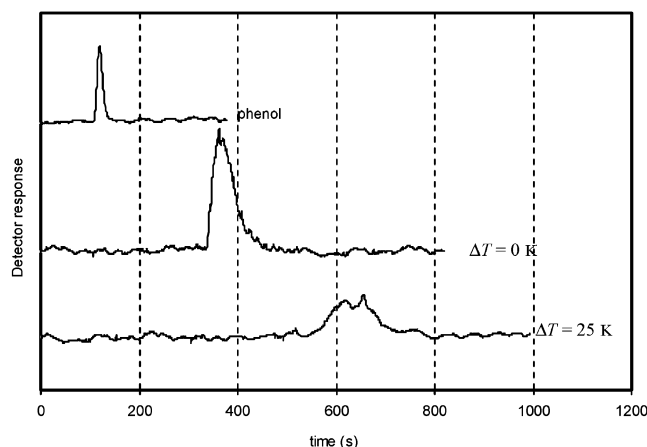


**Figure 2.** Fractograms (detector response in arbitrary units vs time) of phenol, Si-OH particles at  $\Delta T = 0$  K, and Si-OH particles at  $\Delta T = 25$  K in the horizontal thermal FFF channel (from top to bottom). Carrier liquid: acetonitrile. Carrier flow rate: 0.5 mL/min.  $T_c = 293$  K.

porous particles used as packing materials for liquid chromatography, with a nominal pore size of 120 Å, a specific surface area of 170 m<sup>2</sup> g<sup>-1</sup>, and a specific pore volume of 0.69 cm<sup>3</sup> g<sup>-1</sup>. The Hypersil particles are silica particles used for normal-phase liquid chromatography. The Hypersil-ODS particles are silica-based particles bonded with octadecylsilane groups, used for reverse-phase liquid chromatography. These particles can be considered as non-Brownian, as their Peclet number (see above) in water is about 50.

Both types of particles were suspended in acetonitrile (SDS, Peypin, France). In addition, experiments were performed with the silica (Si-OH) particles suspended in deionized water and with the silica-ODS (Si-ODS) particles suspended in *n*-heptane (SDS, Peypin, France), in all cases at a concentration of 1% (w/v). This value was found to be a good compromise between detector sensitivity and absence of overloading and aggregation effects. No additive (salt or surfactant) was added to the suspending liquid. All suspending liquids were degassed before use in thermal FFF to prevent bubble formation.

For each set of particle-carrier system and each value of the temperature difference,  $\Delta T = T_h - T_c$ , across the thermal FFF channel, experiments were performed in triplicate. When appropriate, the mean values of the experimentally measured parameters are reported with error bars corresponding to plus or minus one standard deviation.

## Results and Discussion

The record of the detector signal as a function of time elapsed since sample injection in the FFF channel is called a fractogram. When a single species is injected in the carrier liquid, the fractogram represents the residence time distribution of this species in the channel. The fractograms obtained, with the same carrier flow rate, for the Si-OH particles in acetonitrile with and without a temperature difference across the horizontally oriented thermal FFF channel are shown in Figure 2. Also shown in this figure is the fractogram of phenol, an unretained solute, which serves as a marker for void time,  $t_0$ , i.e., for the mean residence time of the carrier liquid in the channel (computed as the first moment of the residence time distribution of this compound).<sup>42</sup> As discussed above, the elution time of the particles at  $\Delta T = 0$  K is significantly larger than that of the phenol peak. This reflects the fact that, in the horizontal channel configuration, particles are retained due to the interplay of gravitational and hydrodynamic lift forces, in the so-called lift

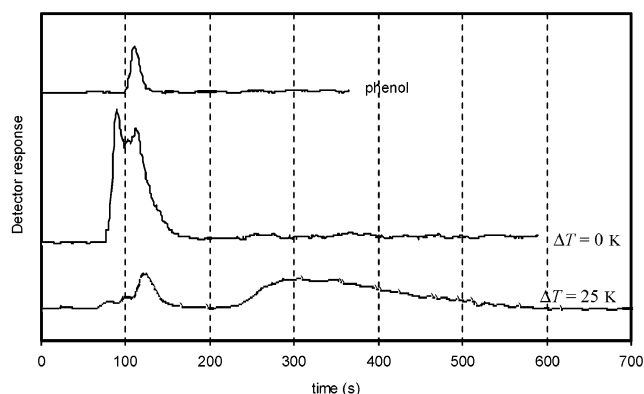


**Figure 3.** Fractograms (detector response in arbitrary units vs time) of phenol, Si-ODS particles at  $\Delta T = 0$  K, and Si-ODS particles at  $\Delta T = 25$  K in the vertical thermal FFF channel (from top to bottom). Carrier liquid: acetonitrile. Carrier flow rate: 0.5 mL/min.  $T_c = 293$  K.

retention mode.<sup>43</sup> When a temperature gradient was applied, the elution time of the particles was noticeably larger, which seems to indicate that particles are sensitive to the application of the temperature gradient. However, on repeating the experiment, large fluctuations in the particle retention time (defined as the mean residence time) were noticed from run to run, even when no temperature gradient was applied. Similar difficulties in obtaining reproducible results have also been noticed by other researchers. Since the amplitude of these fluctuations was of the same order of magnitude as the difference in the elution times observed in Figure 2 for particles with and without  $\Delta T$ , a definitive conclusion about particle thermophoresis cannot be drawn.

Furthermore, an incomplete recovery of the injected samples in the successive experiments was noted. Disassembling the channel revealed that particles had remained accumulated at the bottom plate. To check whether this could be a result of the nickel nature of the plating of the copper walls of the channel used in this study, experiments with the same Si-OH particles were performed in the chromium-plated thermal FFF channel used at the University of Ferrara (Italy) and described by Contado et al.<sup>44</sup> The results were similar, characterized by a poor reproducibility, partial sample recovery, and particle deposition at the bottom cold plate.

### Evidence of Thermophoresis of Non-Brownian Particles.

Suspecting an adverse role played by the sedimentation of the particles toward the bottom plate on reproducibility and retention, we decided to decouple the eventual action of thermophoresis on particles from that of gravity by orienting vertically the FFF channel. The results obtained for the Si-ODS particles suspended in acetonitrile and for phenol are shown in Figure 3. They are markedly different from those of Figure 2. At  $\Delta T = 0$  K, the elution time of the particle peak is similar to that of phenol. Furthermore, at  $\Delta T = 25$  K, a well-retained peak, with an elution time much larger than the void time, is observed. Since gravity acts in the flow direction rather than in the field direction, this difference in peak behavior is attributable to the sole action of the temperature gradient on the particles. As the reproducibility of the retention time of the retained particle peak is much better than in the horizontal channel configuration (variations are about 1%), this allows us to positively conclude about the existence of thermophoresis for these non-Brownian particles in pure acetonitrile. The results of Figure 3 were obtained for an upward carrier flow. Experiments performed with a downward carrier flow produced very similar results.

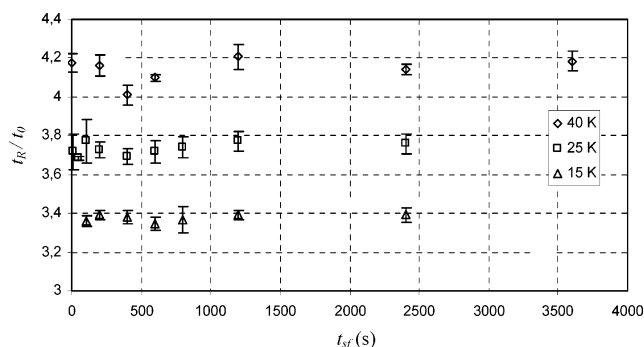


**Figure 4.** Retention time,  $t_R$ , of Si-ODS particles in acetonitrile, relative to the void time,  $t_o$ , vs duration,  $t_{sf}$ , of the stop-flow period, for different values of the temperature drop  $\Delta T$  in vertical channel. Upward flow rate: 0.5 mL/min.  $T_c = 293$  K. From bottom to top:  $\Delta T = 15$  K, 25 K, 40 K.

As seen in Figure 3, the fractogram of the Si-ODS particles for  $\Delta T = 25$  K exhibits two peaks: the well-retained peak and another smaller peak near the void time. Quite similar results were obtained for the Si-OH particles. This is a rather general feature observed in FFF of particulate samples. The optical microscopic analysis of the effluent fractions collected during the elution of these two peaks showed that they both contained sample particles of similar sizes. The presence of such a double peak for a given species in an elution system is usually associated with insufficient transverse relaxation after sample injection in the channel.<sup>45</sup> To avoid or limit this phenomenon in FFF, the carrier flow is generally stopped during a certain period just after sample introduction to allow the sample components to approach a steady state distribution in the channel cross-section under the influence of the applied field. This stop-flow operation was performed for the particle samples. Figure 4 illustrates that, whatever the temperature drop  $\Delta T$  applied, the mean elution time,  $t_R$ , of the retained peak of the Si-ODS particles in acetonitrile, after resuming carrier flow, does not depend on stop-flow duration,  $t_{sf}$ . It is seen that the retention time of the particles increases with  $\Delta T$ . This can be explained by the fact that the stronger thermophoretic force acting on particles at larger  $\Delta T$  pushes them closer to the accumulation wall where the flow streamlines have a lower velocity than farther away from the wall.

For each particle-carrier system, each  $\Delta T$ , and each value of the stop-flow duration, we measured the ratio,  $F_R$ , of the area,  $A_R$ , of the retained peak to the sum,  $A_{tot}$ , of the areas of the nonretained and retained particle peaks. In Figure 5 are plotted the values of  $F_R$  measured as a function of  $t_{sf}$  for Si-ODS particles in acetonitrile and three different values of  $\Delta T$ . For  $\Delta T = 15$  K, it is seen that  $F_R$  first increases with  $t_{sf}$ , then, after a threshold value,  $t_{thres}$ , remains approximately constant with further increase of the stop-flow duration. Similar variations are also noticed for larger  $\Delta T$ , but the range of variations of  $F_R$  with  $t_{sf}$  becomes smaller as  $\Delta T$  increases. The total area,  $A_{tot}$ , was observed to be uncorrelated to the stop-flow duration and to be nearly constant (its coefficients of variation, for the triplicate experiments performed at all  $t_{sf}$  values, were in the range 7–9% for the various sets of particle type, carrier, and  $\Delta T$ ). This indicates that particles did not adsorb on or adhere to the channel walls.

The value of  $F_R$  is associated with the concentration distribution of the particles across the channel at the end of the stop-flow period, when the carrier flow is resumed. The deviation of  $F_R$  from unity, even at long stop-flow durations, has a hydrodynamic origin. The investigation of the migration mechanism is beyond the scope of the present study and will be

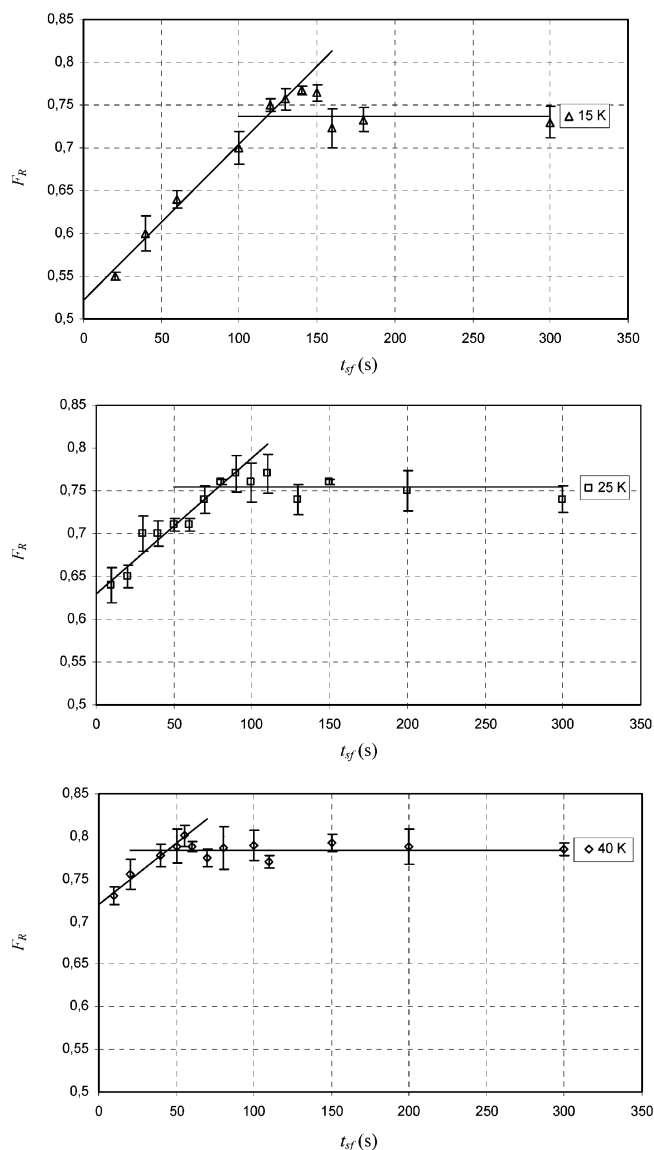


**Figure 5.** Fractional area of retained peak,  $F_R$ , for Si-ODS particles in acetonitrile vs duration,  $t_{sf}$ , of the stop-flow period, for different values of the temperature drop  $\Delta T$  in vertical channel. Upward flow rate: 0.5 mL/min.  $T_c = 293$  K. From top to bottom:  $\Delta T = 15$  K, 25 K, 40 K.

discussed in a forthcoming publication. Nevertheless, for the present purpose, it can be considered, in first approximation, that the amount of particles present in the retained peak is linearly related to the number of particles located at the accumulation wall, or very close to it, at the end of the stop-flow procedure. The only physical effect affecting the particle behavior during the stop-flow period is the transversal migration induced by thermophoresis. Indeed, gravity has a negligible effect, since, in 150 s, a time greater than the observed  $t_{thres}$  values, it leads to a vertical displacement of, at most, 1.5 mm, which is negligible in comparison with the channel length. Hence, the variations of  $F_R$  with  $t_{sf}$  provide information on the kinetics of the thermophoretic process.

The evolution of the concentration profile across the channel thickness during the stop-flow procedure, while the particles are displaced toward the accumulation wall by thermophoresis, is analogous to that observed during the transient sedimentation of an initially uniform suspension of identical non-Brownian particles. During the sedimentation of a dilute suspension, a sharp front separates the upper clear liquid from the suspension in the lower part of the vessel where the concentration remains



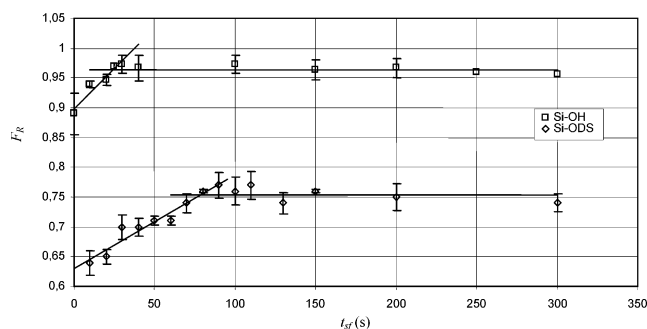


**Figure 6.** Fractional area of retained peak,  $F_R$ , for Si-OH (upper curve) and Si-ODS (lower curve) particles in acetonitrile vs duration,  $t_{sf}$ , of the stop-flow period in vertical channel. Upward flow rate: 0.5 mL/min.  $T_c = 293$  K. Temperature drop:  $\Delta T = 25$  K.

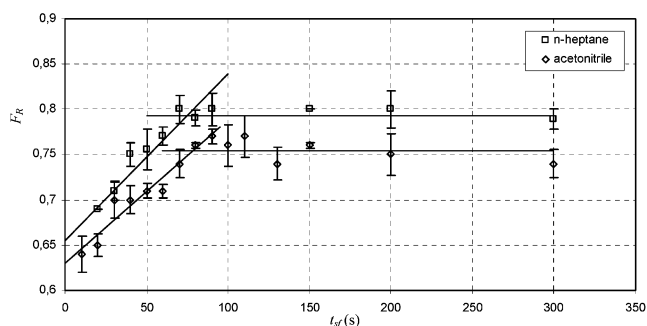


**Figure 7.** Fractional area of retained peak,  $F_R$ , for Si-ODS particles in *n*-heptane (upper curve) and acetonitrile (lower curve) vs duration,  $t_{sf}$ , of the stop-flow period in vertical channel. Upward flow rate: 0.5 mL/min.  $T_c = 293$  K. Temperature drop:  $\Delta T = 25$  K.

uniform and equal to the initial concentration. This front moves downward at the particle sedimentation velocity.<sup>46</sup> Hence the amount of particles deposited on the accumulation wall increases linearly with time until the front reaches the wall, and then remains constant. Therefore, one expects that, in a thermal FFF experiment with non-Brownian particles, the relative area,  $F_R$ , of the retained particle peak increases linearly with  $t_{sf}$ , until the threshold time,  $t_{thres}$ , at which time the thermophoretic front, separating the clear liquid from the suspension, reaches the accumulation wall. Then, for  $t_{sf} > t_{thres}$ , it remains approximately constant, as all particles are deposited at the accumulation wall. Hence the clear existence of a threshold time observed in Figure 5 for  $\Delta T = 15$  and 25 K provides evidence of the existence of thermophoresis for these non-Brownian particles in pure liquids.

As seen in Figure 5, the value of  $t_{thres}$  decreases with increasing  $\Delta T$ . Figure 6 shows that, for a given  $\Delta T$  and a given suspending liquid, here acetonitrile, it also depends on the nature of the particles and is larger for Si-ODS than for Si-OH particles. Finally, Figure 7 shows that for Si-ODS particles, at a given  $\Delta T$ , the threshold time is not statistically different in acetonitrile and in *n*-heptane. In the case of Si-OH particles,  $t_{thres}$  values are slightly lower in water than in acetonitrile.

**Estimation of the Thermophoretic Mobility.** This interpretation of the shape of the  $F_R$  versus  $t_{sf}$  curves described above provides a method for estimating the thermophoretic velocity and the thermophoretic mobility of non-Brownian particles. Indeed, the threshold time is regarded as the time at which the thermophoretic front reaches the accumulation wall, i.e., as the time required for the migration of the particles across the channel thickness by thermophoresis. This allows the expression of the particle thermophoretic velocity,  $U_T$ , as

$$U_T = \frac{w - d}{t_{thres}} \quad (1)$$

where  $w$  is the channel thickness and  $d$  the particle diameter,  $w - d$  being the transversal migration distance in time  $t_{thres}$ , taking into account the steric exclusion of the particles from the walls. The thermophoretic force,  $F_T$ , is given as

$$F_T = 3\pi\eta d U_T = 3\pi\eta \frac{d(w - d)}{t_{thres}} \quad (2)$$

where  $\eta$  is the carrier viscosity. As  $D_T$  is defined as the thermophoretic velocity per unit value of the temperature gradient,  $\Delta T/w$ , one gets

$$D_T \equiv \frac{U_T}{\Delta T/w} = \frac{(w - d)w}{t_{thres}\Delta T} \quad (3)$$

The accuracy of the determinations of  $U_T$ ,  $F_T$ , and  $D_T$  relies on that of  $t_{thres}$ . For each set of particle type, carrier, and  $\Delta T$ , the data of  $F_R$  experiments were performed in triplicate at  $n$  different  $t_{sf}$  values. To determine  $t_{thres}$ , the  $F_R$  versus  $t_{sf}$  data, where  $F_R$  is the average value of triplicate experiments, were separated in two groups. For the first group, with the lowest  $n_1$   $t_{sf}$  values, a least mean square linear regression analysis was performed. For the second group, the mean of the  $(n - n_1)$  values of  $F_R$  at the largest  $t_{sf}$  was computed to determine the ordinate of the line of zero slope fitting the data at large  $t_{sf}$ . The overall sum of the squares of the residues was calculated. The process was repeated by changing  $n_1$ , keeping  $n_1$  and  $(n - n_1)$  larger than 2. For that optimal value of  $n_1$  that minimizes the sum of the squares of residues,  $t_{thres}$  was determined as the value of  $t_{sf}$  at the intersection between the lines fitting the two groups of data. These regression lines are drawn in Figures 5–7. Several methods are available to determine the confidence interval of their intersection point. We used the method developed by Jandera et al.<sup>47,48</sup> to determine the confidence interval of each  $t_{thres}$  value at the 90% probability level. It slightly overestimates the results of the method described by Miller and Miller.<sup>49</sup>

Since  $D_T$  is an intrinsic property of the particle–liquid system, eq 3 suggests that the product  $t_{thres} \times \Delta T$  does not depend on the applied temperature drop  $\Delta T$ . In Figures 8a and 8b, the product  $t_{thres} \times \Delta T$  is plotted versus  $\Delta T$  for the four particle–liquid systems tested in this study, together with confidence intervals at the 90% probability level. This product is seen to be reasonably constant, taking into account the limited accuracy of the determination of  $t_{thres}$ , except for Si-ODS particles in *n*-heptane at  $\Delta T = 40$  K. This constancy provides a strong confirmation of the validity of the hypothesis made for interpreting  $t_{thres}$ .

When  $t_{sf}$  is smaller than  $t_{thres}$ , the transverse thermophoretic displacement of the particles toward the accumulation is incomplete at the time the flow is resumed. This transverse displacement is then pursued for a time  $t_{thres} - t_{sf}$ , during the migration process along the channel. As discussed above, this is the reason that  $F_R$  differs from its limiting value at large  $t_{sf}$ . One therefore expects that  $\Delta F_R$ , the range of variations of  $F_R$  from  $t_{sf} = 0$  to  $t_{sf} \geq t_{thres}$ , increases with increasing  $t_{thres}/t_R$  ratio. As  $\Delta T$  increases,  $t_{thres}$  decreases, and the retention time increases, as seen in Figure 4. Hence, the  $t_{thres}/t_R$  ratio decreases, and  $\Delta F_R$  decreases, as seen in Figure 5. At  $\Delta T = 40$  K,  $\Delta F_R$  becomes too small, in comparison with the error bars, for clearly observing the transition of the  $F_R$  versus  $t_{sf}$  plots. Consequently,

**TABLE 1: Thermophoretic Mobility,  $D_T$ , Thermophoretic Velocity,  $U_T$ , at  $\Delta T = 25$  K, and Thermophoretic Force,  $F_T$ , at  $\Delta T = 25$  K, for Various Particle–Liquid Systems, and Relative Error on the Determination of These Values at 90% Probability Level ( $\pm\delta$  %)**

	Si-OH/ water	Si-OH/ acetonitrile	Si-ODS/ acetonitrile	Si-ODS/ <i>n</i> -heptane
$D_T$ ( $\text{m}^2 \text{s}^{-1} \text{K}^{-1}$ )	$2.2 \times 10^{-11}$	$1.6 \times 10^{-11}$	$5.2 \times 10^{-12}$	$5.7 \times 10^{-12}$
$U_T$ ( $\text{m s}^{-1}$ )	$5.5 \times 10^{-6}$	$4.0 \times 10^{-6}$	$1.3 \times 10^{-6}$	$1.4 \times 10^{-6}$
$F_T$ (N)	$1.4 \times 10^{-13}$	$3.8 \times 10^{-14}$	$1.3 \times 10^{-14}$	$1.6 \times 10^{-14}$
$\delta$ %	14%	14%	14%	9%

only data obtained at  $\Delta T = 15$  and 25 K were considered for the determination of  $D_T$ . The average  $D_T$  values obtained from measurements at these two  $\Delta T$  values for the four particle–liquid systems are reported in Table 1, as well as the thermophoretic velocities and the thermophoretic forces for  $\Delta T = 25$  K, and the relative errors of all these parameters at the 90% probability level.

#### Comparison with Literature Data on Brownian Particles.

Note that the  $D_T$  values reported in Table 1 correspond to the 3  $\mu\text{m}$  particles used in this study. They may be different for similar micron-sized particles of different diameters, as this has been observed for submicron particles. Although spanning a 4-fold range, these values are on the same order of magnitude as those reported for polymers in organic solutions, which increases the confidence in the method of determination of  $D_T$ . These values are about 1 order of magnitude smaller than the values obtained by McNab and Meisen for PS latex particles suspended in either *n*-hexane or water.<sup>13</sup> Still the latter values are nearly two-orders of magnitude larger than those obtained for PS submicron latex colloids by thermal FFF in aqueous salt or surfactants solutions.<sup>15,16,23,24,50</sup> These particles generally exhibit larger  $D_T$  values in a salt acetonitrile solution than in aqueous solutions<sup>38,50</sup> or when the acetonitrile content of mixtures with water increases.<sup>24</sup>

The  $D_T$  values reported in the thermal FFF literature for Si-OH or Si-ODS submicron particles cannot be straightforwardly compared with data of Table 1 because they were obtained, not in pure liquids, but in aqueous or organic solutions with varying concentrations of salts or surfactants. In aqueous solutions,  $D_T$  values appear to be only slightly dependent on Si-OH particle size and to be in the range of  $(1\text{--}4) \times 10^{-12} \text{ m}^2 \text{s}^{-1} \text{K}^{-1}$ , the value increasing with increasing salt or surfactant concentration.<sup>15,23,50</sup> Instead, in acetonitrile solutions,  $D_T$  has been found to decrease with increasing particle size and the values are, usually but not always, larger than in aqueous solutions.<sup>16,23,50</sup> As concerns Si-ODS submicron particles, only one study reports a  $D_T$  value of  $2.1 \times 10^{-12} \text{ m}^2 \text{s}^{-1} \text{K}^{-1}$  in an aqueous solution.<sup>50</sup> However, it was observed that the retention time of Si-OH particles was significantly lower than that of Si-ODS particles of the same size, which implies that the  $D_T$  value of the latter is larger than that of the former.<sup>17,23</sup> It was also shown that the retention time of Si-ODS particles was similar to that of PS latex colloids of the same size, which implies that their  $D_T$  values are also similar.<sup>17</sup> In light of these results, the  $D_T$  data presented in Table 1 appear to be larger than those reported for submicron particles, noting again that we operated with pure liquids instead of solutions. For this reason, it was not possible to make measurements with Si-ODS particles in water because they aggregate in the absence of surfactant or salt. Although they are not directly comparable, our results for micron-sized silica-based particles in pure liquids differ in two aspects from those of submicron particles in liquid solutions: first,  $D_T$  for Si-OH particles is slightly larger in water than in acetonitrile; second, in acetonitrile,  $D_T$  for Si-OH particles is

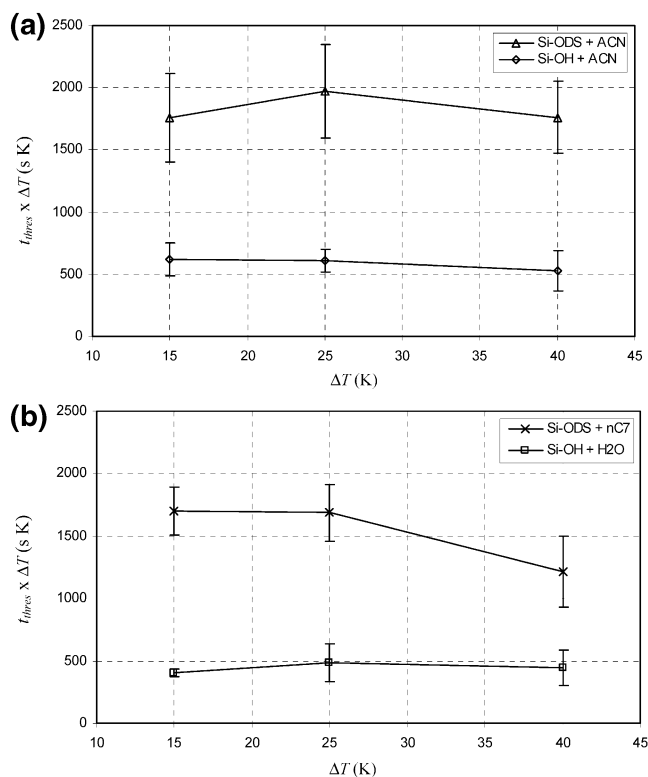


**Figure 8.** Product of the threshold value of the stop-flow duration,  $t_{\text{thres}}$ , and temperature drop,  $\Delta T$ , vs  $\Delta T$ , for the various particle–carrier liquid systems in vertical channel (ACN = acetonitrile; H<sub>2</sub>O = water; nC7 = *n*-heptane). Upward flow rate: 0.5 mL/min.  $T_c = 293$  K. (a) Si-ODS (upper curve) and Si-OH (lower curve) particles in acetonitrile; (b) Si-ODS particles in *n*-heptane (upper curve) and Si-OH particles in water (lower curve).

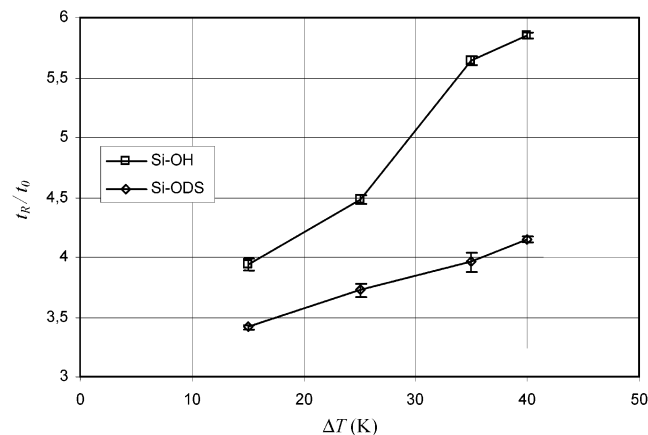


**Figure 9.** Retention time,  $t_R$ , of Si-OH (upper curve) and Si-ODS (lower curve) particles in acetonitrile, relative to the void time,  $t_0$ , vs temperature drop  $\Delta T$  in vertical channel. Upward flow rate: 0.5 mL/min.  $T_c = 293$  K. Stop-flow duration:  $t_{\text{sf}} = 300$  s.

about 3 times larger than for Si-ODS particles. Clearly,  $D_T$  depends on the chemical nature of the particle surface. A further and complementary evidence that the thermophoretic mobility of Si-OH particles is larger than that of Si-ODS particles is provided by Figure 9, which shows that, whatever  $\Delta T$ , the retention time of Si-OH particles is larger than that of Si-ODS particles. This implies that the thermophoresis force acting on the former is stronger. This is in sharp contrast with findings for submicron silica-based particles in aqueous solutions.<sup>17,23</sup> It is not clear whether this comes from the change of the suspending liquid (acetonitrile rather than water), or from the ionic strength of the liquid (pure liquid rather than salt solution),

or, still, from the change of particle size (non-Brownian rather than Brownian particles).

One may attempt to compare the  $D_T$  data reported in Table 1 with the values predicted by Semenov's theory of particle thermophoresis in pure liquids.<sup>37</sup> According to this theory,  $D_T$  is given by

$$D_T = 0.0343 \frac{\alpha_T}{\eta r_o} \frac{\sqrt{A_p A_1}}{2 + \kappa} \quad (4)$$

where  $\alpha_T$ ,  $r_o$ , and  $\eta$  are the thermal expansion coefficient, the molecular radius, and the viscosity of the suspending liquid,  $A_p$  and  $A_1$  are the particle and carrier liquid Hamaker constants, respectively, and  $\kappa$  is the particle-to-liquid thermal conductivity ratio. This theory predicts that  $D_T$  is independent of particle size. The resulting  $D_T$  values for silica particles in water and in acetonitrile are reported equal to  $1.9 \times 10^{-12}$  and  $2.4 \times 10^{-11} \text{ m}^2 \text{ s}^{-1} \text{ K}^{-1}$ , respectively.<sup>37</sup> However, the  $D_T$  values calculated when using the values of the parameters of eq 4 reported in the tables of ref 37 are about 3.5 times smaller. Anyway, the value in water is about 13 times smaller than that of acetonitrile, while in our experiments, it is 1.4 times larger. Still, theoretical and experimental values are of comparable order of magnitude. It should be noted however that in Semenov's theory particles are supposed to be plain, while we used porous particles, with a solid-liquid interfacial area about 180 times larger than that of plain silica particles of the same size. This significant difference in the structure of the particles does not allow the use of our experimental  $D_T$  values to conclude about the validity of Semenov's theory.

The  $D_T$ ,  $U_T$ , and  $F_T$  data reported in Table 1 should be considered as absolute values, as the stop-flow method used to determine them does not provide information on the direction of migration. It has been recently noted that submicron silica particles, like any other colloidal material investigated, are driven by thermophoresis toward the cold wall.<sup>50</sup> McNab and Meisen had also observed, by optical visualization, that their PS particles were driven toward the cold region.<sup>13</sup> Unfortunately, the thermal FFF instrument does not allow optical visualization of the particles inside the channel.

It is interesting to compare the thermophoretic forces reported in Table 1 with the gravitational forces,  $F_g$ , acting on the particles. Taking into account the particle porosity, the  $F_g$  values are equal to  $6.2 \times 10^{-14} \text{ N}$  in water and  $7.5 \times 10^{-14} \text{ N}$  in acetonitrile and *n*-heptane. Thus  $F_g$  is 2–6 times larger than  $F_T$  (for  $\Delta T = 25 \text{ K}$ ) in acetonitrile and *n*-heptane, but more than two times smaller in water. We performed experiments with the channel in the horizontal orientation but with the hot plate at the bottom (as the cold, denser liquid is then at the top, such a configuration should lead to a flow instability; however the critical Rayleigh number for the development of this Kelvin-Helmholtz is far above the operational Rayleigh number because of the very thin channel thickness). In principle, since  $F_T$  and  $F_g$  are of similar order of magnitude, the comparison of retention data between the top hot plate and the bottom hot plate configurations should allow the determination of the sign of the thermophoretic mobility. Indeed, thermophoresis will co-operate with or counteract sedimentation, and thus increase or decrease retention, depending on the sign. However, the large fluctuations in retention time observed prohibited any definitive conclusion about the sign of  $D_T$ .

The method used for determining  $D_T$  relies on the thermophoretic transversal displacement of the particles occurring during the stop-flow period and is based on the fact that this

transport influences the features of the fractogram. It is interesting to note that the use of the transient behavior of a solution when it is submitted to a temperature gradient was already suggested as a method of determination of thermodiffusion parameters.<sup>51</sup>

## Conclusions

In this study, it has been clearly demonstrated that non-Brownian micron-sized particles possess a thermophoretic mobility in pure liquids and a method has been developed to quantitatively estimate the absolute value of this mobility.

The experimental evidence that porous silica-based particles exhibit a thermophoretic mobility and that this mobility depends on the chemical nature of the surface of the particles suggests that thermophoresis may eventually be exploited for characterizing the properties of the surface of non-Brownian particles, such as the type of chemical ligands bonded to the silica material and the extent of bonding.

The method described in this study for the determination of the thermophoretic mobility of the particles is quite general. It can, in principle, be applied to the determination of the phoretic mobility of non-Brownian particles in other types of applied force fields, such as, the magnetophoretic mobility manifested in a magnetic field.

**Acknowledgment.** Antoine-Michel Siouffi (University of Aix-Marseille 3, France) is gratefully acknowledged for his strong scientific support in this work and for allowing one of us (A.R.) to perform experiments at ESPCI, Paris. We are indebted to Thierry Domenger (Thermo-Electron, Courtabœuf, France) for his generous donation of the Hypersil samples. Francesco Dondi and Catia Contado (University of Ferrara, Italy) are acknowledged for allowing us to perform experiments in their chromium-plated thermal FFF channel under the Galileo 2000 French-Italian governmental program. Alain Jardy (ESPCI, Paris) is gratefully acknowledged for discussions and advice on the determination the confidence intervals of experimental parameters.

## References and Notes

- (1) Ludwig, C. *Sitzungsber. Kaiserl. Akad. Wiss., Math.-Naturwiss. (Vienna)* **1856**, 20, 539.
- (2) Soret, C. *Arch. Sc. Phys. Nat.* **1879**, 3, 48.
- (3) Soret, C. *Arch. Sc. Phys. Nat.* **1880**, 4, 209.
- (4) Soret, C. *Ann. Chim. Phys. 5ème Sér.* **1881**, 22, 293.
- (5) Chapman, S.; Dootson, F. W. *Philos. Mag.* **1917**, 33, 248.
- (6) Debye, P.; Bueche, A. M. In *High-Polymer Physics*; Robinson, H. A., Ed.; Chemical Publishing Co.: Brooklyn, 1948; p 497.
- (7) Clusius, K.; Dickel, G. *Naturwissenschaften* **1938**, 26, 546.
- (8) Clusius, K.; Dickel, G. *Naturwissenschaften* **1939**, 27, 148.
- (9) Giddings, J. C. *Sep. Sci.* **1966**, 1, 123.
- (10) Giddings, J. C.; Hovingh, M. E.; Thompson, G. H. *J. Phys. Chem.* **1970**, 74, 4291.
- (11) Martin, M.; Van Batten, C.; Hoyos, M. In *Thermal Nonequilibrium Phenomena in Fluid Mixtures*; Köhler, W., Wiegand, S., Eds.; Lecture Notes in Physics 584; Springer: Berlin, 2002; p 250.
- (12) Schimpf, M. E. *J. Liq. Chromatogr. Relat. Technol.* **2002**, 25, 2101.
- (13) McNab, G. S.; Meisen, A. *J. Colloid Interface Sci.* **1973**, 44, 339.
- (14) Liu, G.; Giddings, J. C. *Anal. Chem.* **1991**, 63, 296.
- (15) Liu, G.; Giddings, J. C. *Chromatographia* **1992**, 34, 483.
- (16) Shiundu, P. M.; Liu, G.; Giddings, J. C. *Anal. Chem.* **1995**, 67, 2705.
- (17) Shiundu, P. M.; Giddings, J. C. *J. Chromatogr. A* **1995**, 715, 117.
- (18) Bacri, J.-C.; Cebers, A.; Bourdon, A.; Demouchy, G.; Heegard, B. M.; Perzynski, R. *Phys. Rev. Lett.* **1995**, 74, 5032.
- (19) Alves, S.; Demouchy, G.; Bee, A.; Talbot, D.; Bourdon, A.; Figueiredo Neto A. M. *Philos. Mag.* **2003**, 83, 2059.
- (20) Blums, E.; Odenbach, S. *Int. J. Heat Mass Transfer* **2000**, 43, 1637.
- (21) Ratanathanawongs, S. K.; Shiundu, P. M.; Giddings, J. C. *Colloids Surf., A* **1995**, 105, 243.

- (22) Shiundu, P. M.; Remsen, E. E.; Giddings, J. C. *J. Appl. Polym. Sci.* **1996**, *60*, 1695.
- (23) Jeon, S. J.; Schimpf, M. E.; Nyborg A. *Anal. Chem.* **1997**, *69*, 3442.
- (24) Mes, E. P. C.; Kok, W. Th.; Tijssen, R. *Chromatographia* **2001**, *53*, 697.
- (25) Shiundu, P. M.; Munguti, S. M.; Williams, S. K. R. *J. Chromatogr. A* **2003**, *983*, 163.
- (26) Mes, E. P. C.; Tijssen, R.; Kok, W. Th. *J. Chromatogr. A* **2001**, *907*, 201.
- (27) Epstein, P. S. *Z. Phys.* **1929**, *54*, 537.
- (28) Anderson, J. L. *Annu. Rev. Fluid Mech.* **1989**, *21*, 61.
- (29) Ruckenstein, E. *J. Colloid Interface Sci.* **1981**, *83*, 77.
- (30) Giddings, J. C.; Shiundu, P. M.; Semenov, S. N. *J. Colloid Interface Sci.* **1995**, *176*, 454.
- (31) Semenov, S. N. *Colloid J.* **1997**, *59*, 488.
- (32) Semenov, S. N. *J. Microcolumn Sep.* **1997**, *9*, 287.
- (33) Semenov, S. N. *J. Liq. Chromatogr. Relat. Technol.* **1997**, *20*, 2687.
- (34) Schimpf, M. E.; Semenov, S. N. *J. Phys. Chem. B* **2001**, *105*, 2285.
- (35) Morozov, K. I. In *Thermal Nonequilibrium Phenomena in Fluid Mixtures*; Köhler, W., Wiegand, S., Eds.; Lecture Notes in Physics 584; Springer: Berlin, 2002; p 39.
- (36) Bringuier, E.; Bourdon, A. *Phys. Rev. E* **2003**, *67*, 011404.
- (37) Semenov, S. N. *Philos. Mag.* **2003**, *83*, 2199.
- (38) Shiundu, P. M.; Munguti, S. M.; Williams, S. K. R. *J. Chromatogr. A* **2003**, *984*, 67.
- (39) Petersen, R. E., II; Myers, M. N.; Giddings, J. C. *Sep. Sci. Technol.* **1984**, *19*, 307.
- (40) Martin, M. In *Particle Size Analysis 1985*; Lloyd, P. J., Ed.; Wiley: New York, 1987; p 65.
- (41) Van Batten, C.; Hoyos, M.; Martin, M. *Chromatographia* **1997**, *45*, 121.
- (42) Martin, M.; Garcia-Martin, S.; Hoyos, M. *J. Chromatogr. A* **2002**, *960*, 163.
- (43) Martin M. In *Advances in Chromatography*; Brown, P. R., Grushka, E., Eds.; Marcel Dekker: New York, 1998; Vol. 39, p 1.
- (44) Contado, C.; Martin, M.; Dondi, F.; Melucci, D. *Chromatographia* **2002**, *56*, 495.
- (45) Krishnamurthy S.; Subramanian, R. S. *Sep. Sci.* **1977**, *12*, 347.
- (46) Bacri, J.-C.; Frénois, C.; Hoyos, M.; Perzynski, R.; Rakotomalala, N.; Salin, D. *Europhys. Lett.* **1986**, *2*, 123.
- (47) Jandera, P.; Kolda, S.; Kotrlý, S. *Talanta* **1970**, *17*, 443.
- (48) Liteanu, C.; Rica, I. *Statistical Theory and Methodology of Trace Analysis*; Ellis Horwood: Chichester, 1980; p 166.
- (49) Miller, J. N.; Miller, J. C. *Statistics and Chemometrics for Analytical Chemistry*, 4th ed.; Prentice-Hall: Pearson Education Ltd, Harlow, 2000; p 135.
- (50) Shiundu, P. M.; Williams, P. S.; Giddings, J. C. *J. Colloid Interface Sci.* **2003**, *266*, 366.
- (51) De Groot, S. R. *Thermodynamics of Irreversible Processes*; North-Holland Publishing: Amsterdam, 1963; p 116.